David C. Kombo
Matthew A. Young*
David L. Beveridge
Department of Chemistry and Molecular Biophysics Program, Hall-Atwater Laboratory, Wesleyan University, Middletown, CT 06457

Received 20 November 1997; accepted 10 December 1999

One Nanosecond Molecular Dynamics Simulation of the N-Terminal Domain of the λ Repressor Protein

Abstract: *We have carried out molecular dynamics simulation of the N-terminal domain of the λ repressor protein in a surrounding environment including explicit waters and ions. We observe two apparent dynamics substates in the nanosecond protein simulation, the transition occurring around 500 ps. The existence of these two apparent substates results from a high flexibility of the arm in each monomer, a relative flexibility of both arms with respect to each other, and a relative displacement of the recognition helices from 30 to 40 Å of interhelical distance. Many amino acid residues, including those involved in DNA recognition, undergo a simultaneous transition in their side-chain conformations, consistent with the relationship between side-chain conformation and secondary structural elements, as observed in protein crystal structures. This result suggests plausible conformational changes experienced by the protein upon DNA binding. On the whole, the non-consensus monomer appears to be more flexible than its consensus counterpart.* © 2000 John Wiley & Sons, Inc. Biopoly 53: 596–605, 2000

Key words: *molecular dynamics; Monte Carlo simulation; N-terminal; λ-repressor protein; protein–DNA interactions*

INTRODUCTION

Occurrence of protein–DNA interactions is an essential feature of many important physiological events such as DNA synthesis, gene regulation, RNA synthesis, transposition, recombination, and DNA packaging. In an attempt to investigate the molecular basis of protein–DNA interactions and its relevant link to the broader issue of protein design, the λ repressor–operator system has been the object of numerous studies.[1,2] Binding of the λ repressor protein to its DNA operator occurs primarily in a lock and key manner through shape and electronic complementarity of the helix–turn–helix unit (residues 33–51 in each monomer), while an induced fit by means of the N-terminal flexible arm (residues 1–5 in each monomer) also brings its contribution.[3–5] Dimerization of the λ-repressor protein is required for its DNA-binding activity.[3,6]

Correspondence to: David L. Beveridge
Contract grant sponsor: National Institute of Health
Contract grant number: GM-37909
**Present address:* Laboratories of Molecular Biophysics, Howard Hughes Medical Institute, the Rockefeller University, 1230 York Avenue, New York, NY 10021
Biopolymers, Vol. 53, 596–605 (2000)

Although numerous investigations have provided a great deal of information on protein folding, stability, and macromolecular recognition about the λ repressor,[2] the following questions still remain unanswered: (1) Though the λ repressor dimer is made of identical subunits, it recognizes the pseudo-twofold symmetric operator asymmetrically.[7] It has been proposed that the asymmetric binding pattern is due to the difference in geometry. However, it is not clear why such a rather small difference in geometry yields amazingly large differences in binding specificity, with the consensus monomer interacting more strongly than its counterpart non-consensus monomer. (2) Some mutants with substitution at the dimer interface show increased dimerization properties, but reduced DNA-binding activity.[8] Moreover, some other mutations at the dimer interface significantly perturb differential operator affinity.[9] It has been proposed that conformational changes in the tertiary and/or quaternary structure of the subunits may result in placing the recognition helix out of register for proper binding. However, a detailed picture of the structural changes and flexibility resulting from a rigid-body movement of the subunits and coupling between the recognition elements (helix–turn–helix unit and flexible N-terminal arms) is still lacking. (3) Although the structure of the λ protein–DNA complex has been determined at high resolution,[10] the crystal structure of the free λ-repressor protein was only solved at low resolution 10 years earlier.[3] In this structure, only coordinates of C^{α} atoms are available. The lack of side-chain atoms coordinates hinders us from understanding the protein conformational adaptability, which occurs upon DNA binding. (4) Even in the high-resolution crystal structure of the protein–DNA complex, the structure of the flexible N-terminal arm in the non-consensus monomer was not solved.[10] It is not known, for that matter, to which extent the interactions mediated by this N-terminal flexible arm are coupled to those mediated by the helix–turn–helix unit. Moreover, the extent to which the protein–DNA interface can undergo reorganization is still a matter of queries.[11] (5) Previous computational studies on the λ system have at least neglected either hydration and/or salt effects,[12–16] or the dynamic nature of the macromolecular association.[17–19] It is important that an MD simulation of this system be carried out with explicit water molecules and ions, in an attempt to better mimic the physiological environmental conditions and shed light to the above-mentioned questions. This is the specific aim of the work described herein.

METHODS

We have used the AMBER 4.1 macromolecular computer package for energy minimization and dynamics simulation.[20] The starting configuration used in the dynamics simulation was the lowest energy conformation of the system protein-ions obtained from a Monte Carlo (MC) simulation of the ion atmosphere around the λ-repressor protein, as fully described elsewhere.[21] This Monte Carlo generated low-energy conformation was then solvated with 6042 TIP3P water molecules, using a protein box size of $73 \times 59 \times 56$ Å.[3] Each protein monomer has 12 negatively and 13 positively charged amino acid residues at physiological pH. The protonation states for charged residues were determined based on their ionization states at pH 7.0. Thus, charges for Glu and Asp were set to −1e and those for Lys and Arg to +1e. No His residue is found in the N-terminal domain of the λ repressor protein. Prior to the MC simulation, Na^+ and Cl^- ions were added in both monomers of the energy-minimized structure, in the proximity of the side-chain atoms of Glu and Asp, and Lys and Arg, respectively using Cornell et al.'s force field[19] edit module. To ensure electroneutrality of the overall system at pH 7.0, the system included 24 Na^+ and 26 Cl^- ions for the whole protein dimer instead of only 2 Cl^-. This was done to provide an unbiased model of charge neutralization, i.e., the protein has a choice in MC and molecular dynamics (MD) to achieve whatever degree of local charge neutrality it wishes by utilizing either amino acid internal charges or external salt ions. Including only 2 negative charges would force the model toward internal compensation and possibly torque the structure. The MD simulation protocol used has been described in details elsewhere.[22,23] Basically, we used the Particle Mesh Ewald method to treat the electrostatics, a 9 Å cutoff, constant pressure, SHAKE[24] on hydrogens, a 2 fs time step, a temperature of 300 K with Berendsen temperature coupling, and the nonbonded pair list was updated every 10 steps. Six rounds of energy minimization were performed prior to the simulation by varying the restraints imposed on the ions and protein atoms. Likewise, restraints were also imposed during the heating and equilibration stages. Results were analyzed using the Molecular Dynamics Tool Chest (MDTC 2.0) analysis software[25] and the InsightII[26] analysis and decipher modules on a silicon graphics workstation. Helicoidal parameters of the DNA-recognition helix–turn–helix unit (hth) of various DNA-binding proteins homologous to the λ-repressor protein, were calculated and compared to the corresponding values of the MD-averaged structures, obtained within 100–200, 200–300, . . . 900–1000 ps, respectively. The crystal structures of the hth of the following proteins were used: the λ-repressor in complex with the operator OL1,[10] a λ-repressor mutant in complex with OL1,[27] the 434 repressor in complex with OR1,[28] OR2,[29] and OR3,[30] respectively, CAP[31] and Trp[32] repressor proteins in complex with DNA.

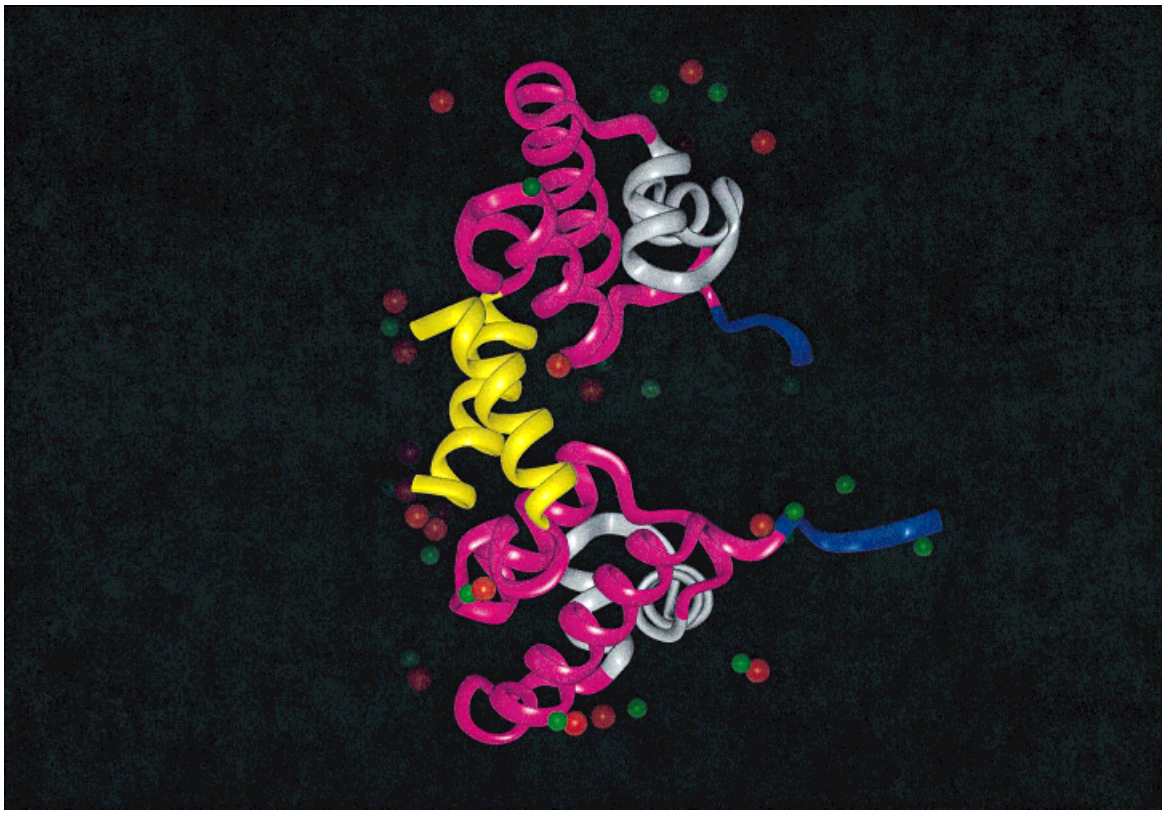

FIGURE 1 Monte Carlo-derived lowest energy configuration of the Na^+ ions (red) and Cl^- ions (green) around the N-terminal domain of the λ repressor protein. The N-terminal arms (residues 1–5) are shown in blue. The helix–turn–helix unit in both monomers is shown in silver. The helix-5 and helix-5′, which mediate the dimerization process, are shown in yellow.

RESULTS

RMS Deviation

Protein Dimer. The lowest energy configuration obtained from the Monte Carlo simulation of the system protein-ions is shown in Figure 1. As described in the Methods section, this configuration was solvated and subsequently used as the starting configuration in the molecular dynamics simulation. We have monitored the stability and convergence of the molecular dynamics simulation by plotting the time evolution of the root mean square deviation of all and backbone atoms of the protein dimer, in one dimension (Figure 2) and two dimensions (Figure 3). The results suggest the presence of two apparent substates, one existing from about 180 to 500 ps and the other one from about 500 ps to 1 ns. The first apparent substate is closer to the starting configuration (≅1.7 Å rms in backbone atoms) than the second one (≅3.2 Å rms in backbone atoms).

To identify the specific portions of the protein, which are responsible for this remarkable jump in the rms deviation, we have carried out a detailed analysis of rms deviations for the functional units of the λ repressor protein. Removal of the N-terminal arms from the protein dimer results in a lowering of the rms deviation, but still confirms the existence of the apparent dynamical substates (Figure 4). Consideration of the arms alone follows the same pattern and results in higher rms, with the values being more elevated for the non-consensus monomer compared to its consensus counterpart (Figure 5). On the whole, the rms deviation of the arms is higher than the one obtained for the rest of the protein; so is the extent of motion observed in the MD trajectory (Figure 6). The rms deviation of the helix–turn–helix units alone, shown in Figure 7, does not exhibit a distinct jump but still shows some high variations between 350 and 700 ps. However, removal of the arms and the helix–turn–helix units from the protein dimer results in a significant disappearance of the apparent two-state trend noticed in the rms (Figure 8). We conclude that the conformational change, which is responsible for this transition in rms deviation, occurs in a concerted

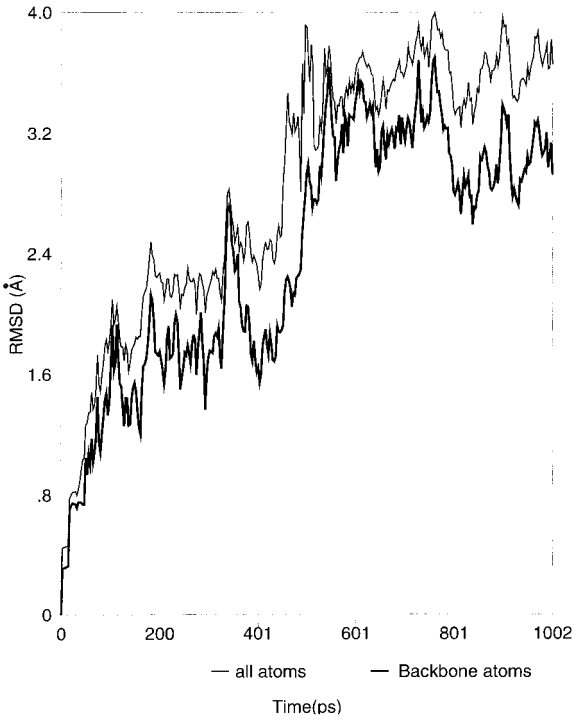

FIGURE 2 The 1D rms deviation for backbone and all atoms of the λ repressor protein dimer, with respect to the starting configuration.

manner between the flexible N-terminal arms and the helix–turn–helix units in the dimer.

Protein Monomers. On the whole, the non-consensus monomer appears more flexible than its consensus counterpart (Figure 9). The rms deviation of the dimer interface helix (helix-5) is also higher in the non-consensus monomer vs the consensus one (data not shown). Likewise, the nonconsensus arm is more flexible than its consensus counterpart (Figure 10). This result is consistent with the fact that the crystallographers have not so far been able to locate the structure of the non-consensus arm in the electron density map. Figure 11 shows that the rms deviation of the helix–turn–helix of each monomer does not exhibit a "two-plateau" pattern. Thus, taken separately, the helix–turn–helix unit in each monomer stays stable during the MD simulation. To validate our results further, we compared the geometrical parameters determined using the Curves computer program[33] for the helix–turn–helix unit of the MD average structure, with those obtained from the analysis of x-ray derived crystal structures of DNA-binding proteins belonging to the λ-repressor family, which are listed in the

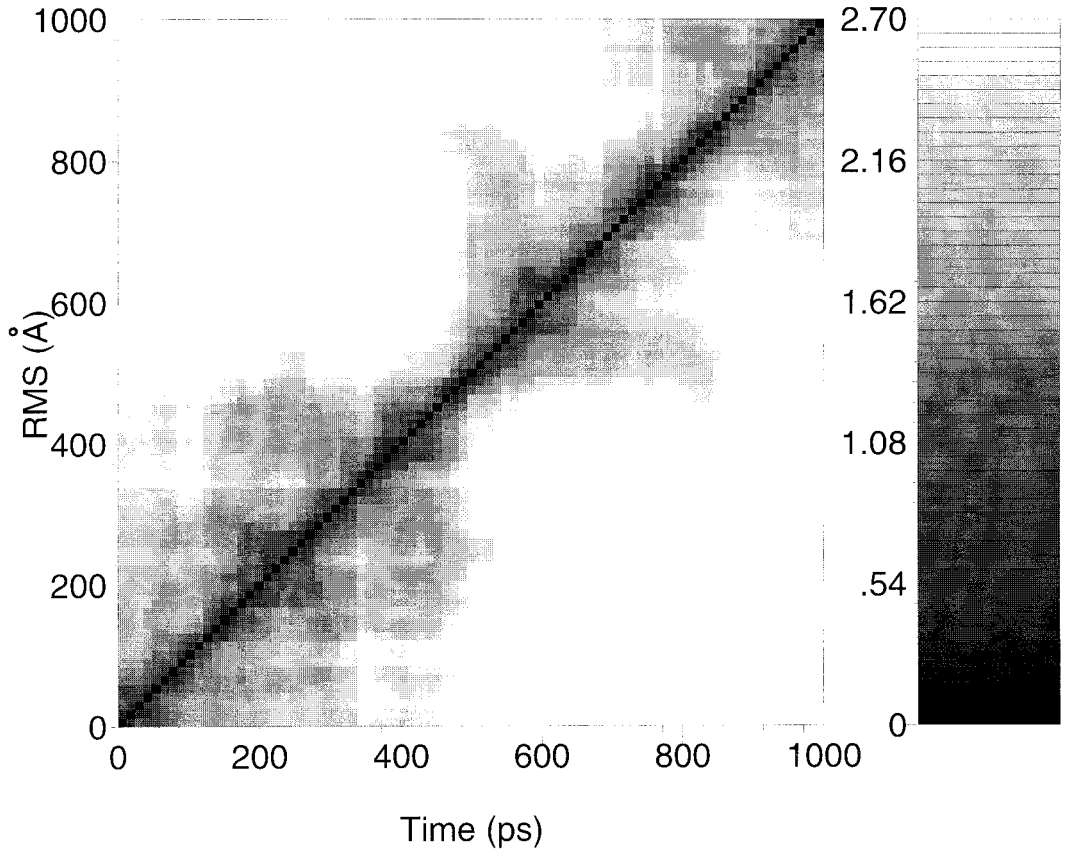

FIGURE 3 The 2D rms deviation map for all atoms of the λ repressor protein dimer.

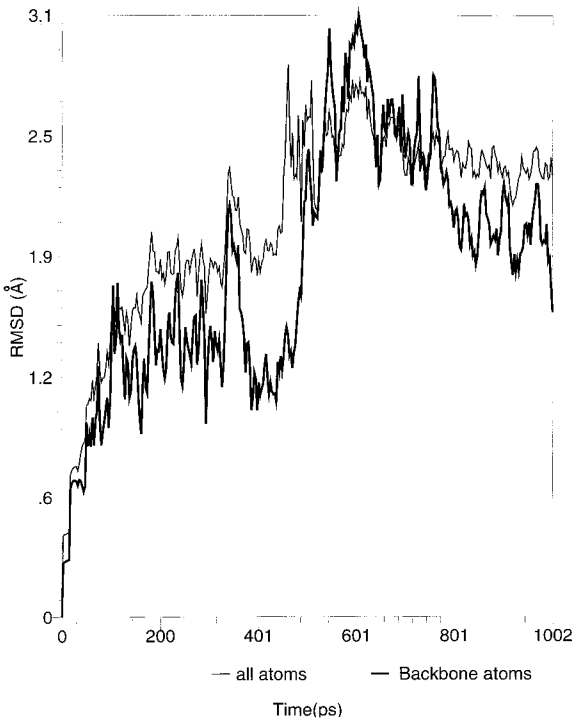

FIGURE 4 The 1D rms deviation for backbone and all atoms of residues 6–92 of both monomers of the repressor protein with respect to the starting configuration. Residues 1–5, which have been excluded, constitute the flexible N-terminal arm.

Methods section. We limited our investigations to the helicoidal parameters twist, rise, Y axis displacement, and tip, which gave regular signatures in characterizing an helix–turn–helix unit. We found that the MD-averaged structures and homologous experimentally observed crystal structures have indistinguishable helicoidal parameters (data not shown). This further supported the stability of our simulation. We conclude that the apparent two-substate behavior discussed so far is also due to the absolute flexibility of each arm in each monomer, but not the absolute behavior of the helix–turn–helix unit, when taken in an isolated context in each monomer.

Conformational Changes

What are the structural changes that are at the origin of the observed jump in rms deviation? Are they restricted to the backbone and side-chain conformation level, or do they also involve the tertiary and quaternary structural elements? To address these questions and characterize the two apparent substates, we have carried out an extensive analysis of all the backbone and side-chain conformations, and relative orientation and distance between α-helical segments.

Side-Chain Dihedral Angles. Table I lists changes in χ^1 dihedral angles only of the residues whose conformations change with the transition in the rms deviation of the protein dimer. We find that the radical changes only involve side-chain dihedral angles (data not shown for χ^2 and χ^3) and occur more frequently in the non-consensus monomer compared to the other monomer.

Interestingly, we observed that the side-chain dihedral angles about the C^{α}–C^{β} bond of a given amino acid residue at a specific location of an α-helix, visited by the substates, take one of the two most observed values at that same specific location in protein crystal structures.[34,35] This result vindicates the idea that the low-energy conformations sampled during our MD simulation are indeed the ones the most observed experimentally and thus provides a further support of the validity of this computational experiment.

Backbone Dihedral Angles. Initial descriptions of the recognition helix (second helix of the helix–turn–helix unit) of the λ-repressor protein, included residues 44–52.[3,4] Later on, the refined structure showed that Asn-52 was not part of the α-helix, because it has $\phi = -100°$ and $\varphi = 13°$.[10] Our MD simulation results show that Asn-52 can actually visit both back-

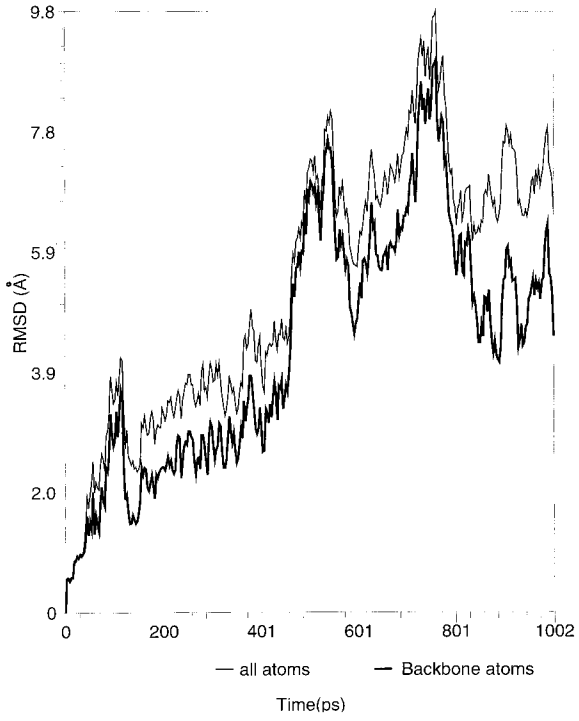

FIGURE 5 The 1D rms deviation for the flexible N-terminal arms in the dimer with respect to the starting configuration.

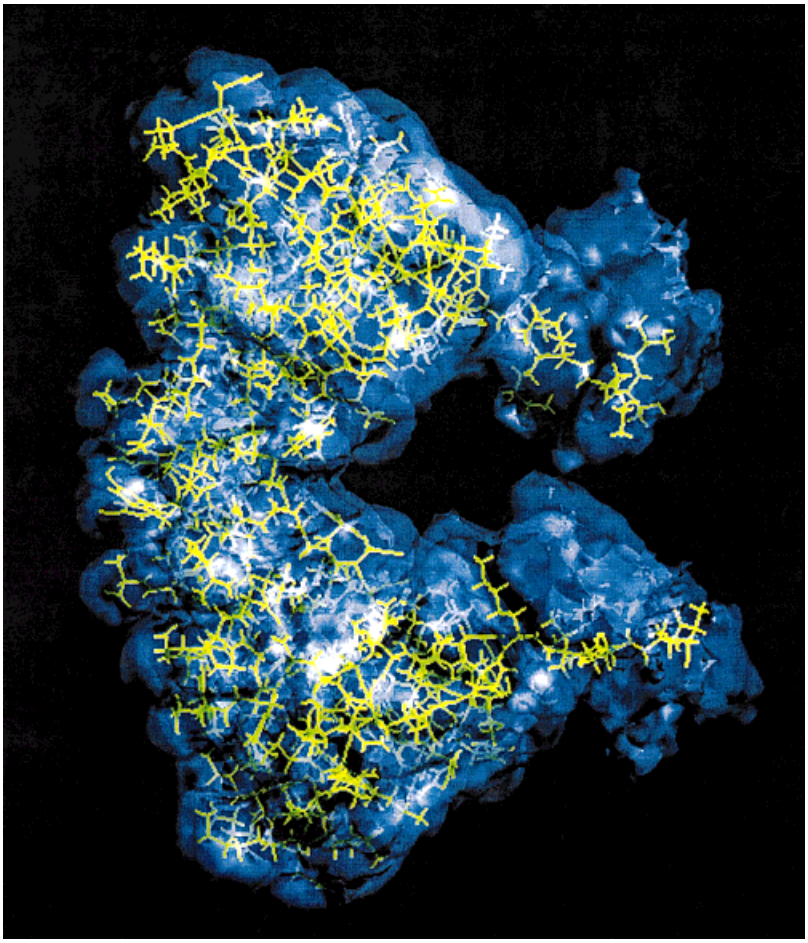

FIGURE 6 Extent of atomic motion encompassing 70% over the entire MD trajectory of the λ-repressor protein dimer.

bone conformations. Table II clearly indicates that this residue has a tendency to adopt an intermediate conformation very close to the 3_{10}-helix ($\phi = -70°$; $\varphi = -18°$) as the simulation time increases. It may be that the recognition helix of the λ repressor protein free in solution includes Asn-52. DNA binding, to which Asn-52 also contributes by making contacts with the DNA sugar phosphate backbone, may alter Asn-52 backbone conformation, thereby shortening the recognition helix such that it ends up including only residues 44–51.

Interhelical Distance of Closest Approach. DNA recognition of proteins with the helix–turn–helix unit requires that the interhelical distance between the recognition helices be about 34 Å, which is approximately the length of a B-DNA turn.[36–38] To investigate whether the backbone and side-chain conformational changes observed in helix-3 (Tables I and II) are accompanied by a significant change in the relative distance between the recognition helices, we followed the time evolution of this geometrical parameter during the simulation. The results, shown in Figure 12, indicate that the closest distance of approach between the recognition helices varies from 30 to 40 Å, while often remaining close to 34 Å. It is interesting to notice that in the vicinity of 500 ps, where there is a transition in the rms deviation, the distance of separation between the recognition helices is reaching its absolute minimum in this nanosecond MD simulation. Separation distances of about 30 Å have also been observed previously in some λ repressor variants in a computational study aimed at discriminating between active and inactive mutants of this protein.[16]

DISCUSSION

Experimental studies have shown that the consensus monomer interacts with the operator more strongly

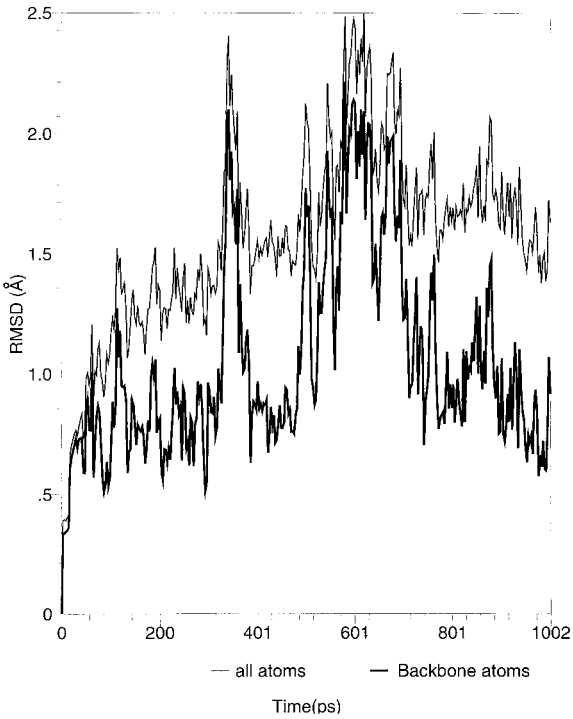

FIGURE 7 The 1D rms deviation for the helix–turn–helix unit in the dimer with respect to the starting conformation.

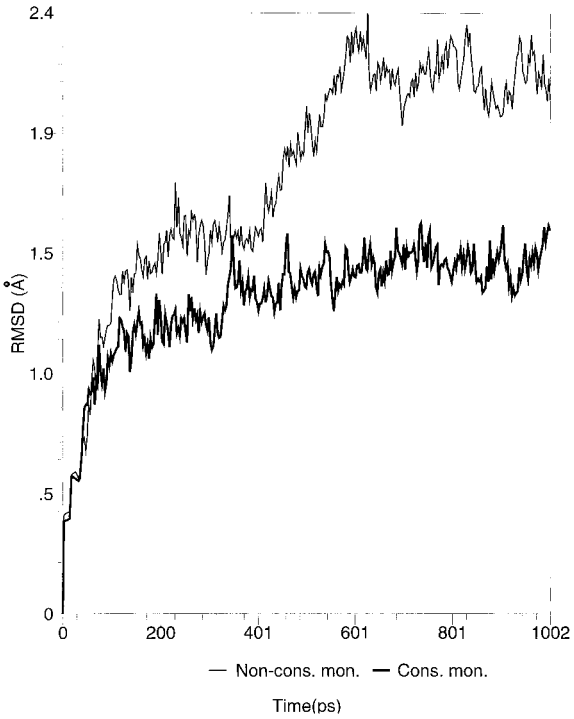

FIGURE 9 The 1D rms deviation of the nonconsensus and consensus monomers, with respect to their respective starting conformations.

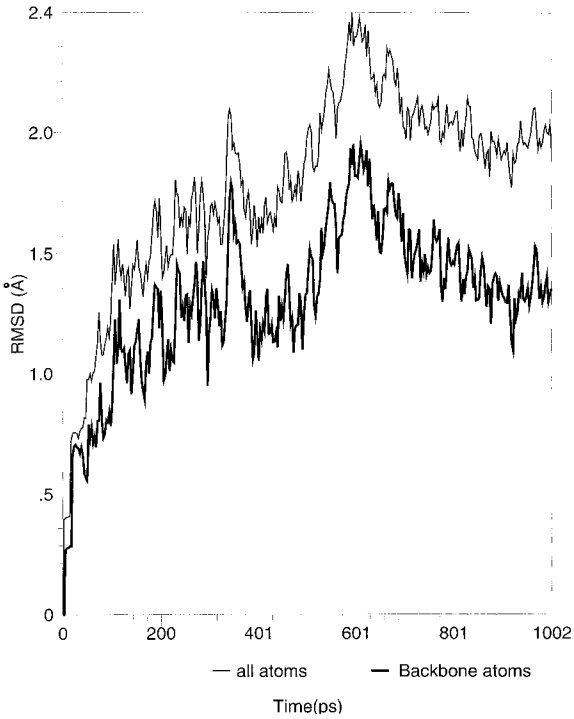

FIGURE 8 The 1D rms deviation for the repressor dimer excluding the arms and the helix–turn–helix unit, with respect to the starting conformation.

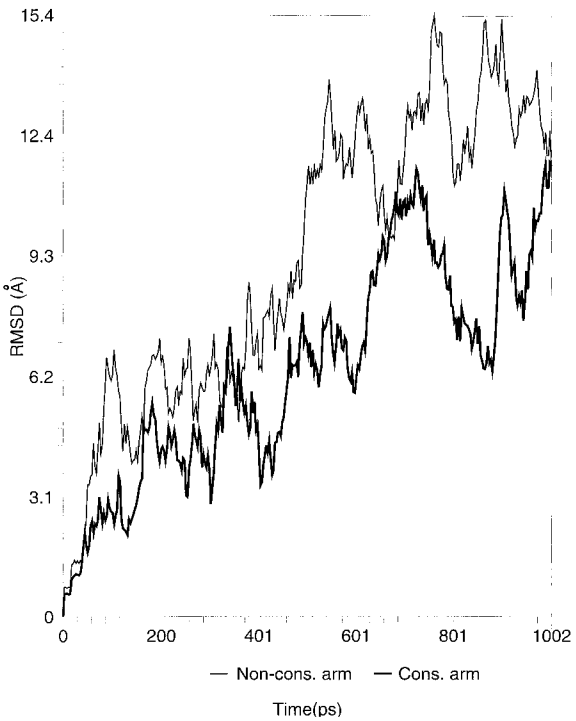

FIGURE 10 The 1D rms deviation of the nonconsensus and consensus N-terminal arms, with respect to their respective starting conformations.

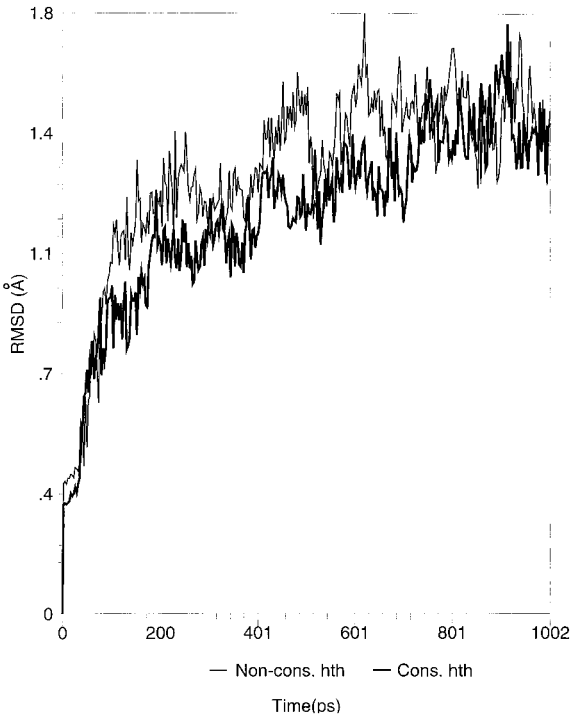

FIGURE 11 The 1D rms deviation of the helix–turn–helix unit of each monomer, with respect to their respective starting conformations.

than its counterpart nonc-onsensus monomer. Our observation that the latter is more flexible than the former suggests that lower extent of local motion in the consensus monomer in the free protein may be necessary in order to reduce the entropic cost of protein–DNA complex formation by induced fit of the flexible N-terminal arm. This is consistent with an MD study on protein–RNA recognition, carried out by Schimmel and his co-workers.[39] They found that critical residues for anticodon-binding activity of class I tRNA synthetase were highly mobile in inactive mutants compared to the active ones.

It is remarkable that the χ^1 dihedral of Ser-1 in the nonconsensus monomer but not in the consensus counterpart, exhibits a transition in the conformational states, going from t to g^+ around the middle of the simulation. Moreover, the observation that the nonconsensus monomer and its N-terminal arm appear to be more flexible than their consensus counterpart may explain the fact that crystallographers have not so far succeeded in observing the electron density map of the nonconsensus N-terminal arm.[3–5,10] It is equally possible that our MD simulation run time was not sufficiently long to allow us to observe a convergence to an identical behavior of the arms in a time-averaged sense, as one would expect given that both monomers have the same chemical identity.

We have observed that the jump in rms deviation is mainly due to the high flexibility of the N-terminal arms and the relative motion of the recognition helices in the dimer. Since this behavior is mainly seen when the rms is determined for the dimer rather than for the monomer per se, we have chosen to call these substates apparent. We have also observed that removal of the arms and the helix–turn–helix unit does not entirely knock out the apparent two-state behavior, as shown in Figure 8. This is due to the fact that some amino acid residues, which belong neither to the arms nor to the recognition helix, still undergo a side-chain conformational change consistent with the rms transition (Table I). Examples include Glu-10, Leu-29, Gln-33, Leu-64, and Ser-79, in the nonconsensus monomer, and Gln-33, Ile-54, and Asn-55, in the consensus monomer. That some of these residues are in close contact with the arm and/or the recognition helix explains the conformational change that results from a structural rearrangement concomitant to the movement of the arms and the recognition helix.

We have observed that some residues involved in DNA-binding exhibit side-chain conformations, which differ from those observed in the DNA-bound conformation (Table I). These side-chain conformations remain the same within 500 ps and are in agreement with the ones observed experimentally in equivalent locations of secondary structural elements. This result demonstrates that molecular dynamic simulation is successfully predicting the preference of amino acid side-chain conformations. However, the lack of knowledge of most of the backbone and all the side-chain atomic positions in the low-resolution free protein structure prevents us from learning unequivocally how well molecular dynamics may predict the experimentally observed free protein structure, when the simulation is started from the DNA-bound protein conformation. We have only superimposed the C^α positions of the MD-derived structures with those of the low-resolution free protein structure and obtained an rms deviation within 3 Å.

The plasticity of the interhelical distance between recognition helices noticed here in the free protein suggests that it is the binding to DNA which forces the protein to adopt the widely observed distance of 34 Å. Moreover, this result suggests that the lambda repressor variant–DNA binding interface might as well be plastic, as observed by Benevides and Weiss.[11] The range of acceptable values for the distance of closest approach between the recognition helices could vary from 30 to 40 Å. In fact, even within the family of DNA-binding proteins that use the helix–turn–helix unit as the recognition motif, the relative orientation of the recognition helices is not the same.[36,37,40]

Table I The χ^1 Side-Chain[a] Conformational Change Accompanying the Transition Observed for the RMS Deviation

Residue	Location[b]	1–500[c]	500–1000[c]	PR[d]	MG[e]	Role[f]
			(a) Non-consensus monomer			
Ser-1	Nter-arm	t	g^+	$g^+\ g^-$	$g^+\ g^- \equiv t$	N
Glu-10	H1, N-end	t	g^-	$g^-\ t$	$g^-\ t$	N
Arg-16	H1, middle	g^-	t	$g^-\ t$	$t\ g^-$	N
Leu-29	Loop, H12	g^-	t	$g^-\ t$	$g^-\ t$	N
Gln-33	H2, N-end	g^-	t	$g^-\ t$	$g^-\ t$	D
Gln-44	H3, N-end	t	g^-	$g^-\ t$	$g^-\ t$	D
Asn-52	Loop, H34	g^-	t	$g^-\ t$	$g^-\ t$	D
Leu-64	H4, N-end	g^-	t	$g^-\ t$	$t\ \ g^-$	N
Ser-79	H5, N-end	g^+	g^-	$g^+\ g^-$	$g^+\ g^-$	N
			(b) Consensus monomer			
Gln-33′	H2′, N-end	g^-	t	$g^-\ t$	$g^-\ t$	D
Ser-45′	H3′, N-end	g^+	g^-	$g^+\ g^-$	$g^+\ g^- \equiv t$	D
Val-47′	H3′, N-end	t	g^+	$t\ \ g^-$	$t\ \ g^+$	C
Ile-54′	Loop, H3′4′	g^-	g^+	$g^-\ g^+$	$g^-\ g^+$	N
Asn-55′	Loop, H3′4′	g^-	t	$g^-\ t$	$g^-\ t$	D

[a] We have adopted the rotamer abbreviations used by Ponder and Richards,[34] which are as follows: g^+, t, and g^- for a χ value centered in the $+60°$ to $+90°$, near 180° and in the $-60°$ to $-90°$ ranges, respectively. Note that these definitions for the g^+ and g^- conformational states are the opposite of the ones used by McGregor.[35]

[b] Hi and loop Hij ($i, j = 1, \ldots, 5$) designates helix-i (one of the five helices of the λ repressor monomer) and the loop between helices i and j. The primed terms regard the consensus monomer.

[c] In picoseconds, designate the first and second half of the nanosecond MD simulation.

[d] From Ponder and Richards.[34] The left and right values represent the first and second most probable rotameric states, respectively.

[e] Same as in footnote d, but from MacGregor.[35]

[f] Biological function of the amino acid residue. The letter codes C, D, and N designate that the residue is conserved within the helix–turn–helix unit containing DNA-binding proteins, involves in DNA recognition, and not known to play a particularly important role, respectively.

CONCLUSIONS

Our observation that two apparent substates exist in the nanosecond MD simulation of the λ-repressor protein reiterates the need for sufficiently long simulations. Furthermore, taken together with the significant variation observed in the distance of closest approach between the recognition helices, this finding prompts us to suggest that local side-chain conformational changes and rigid body shift of the recognition helices may accompany the DNA-binding process. Having to choose among the numerous available conformations and relative interhelical distances observed here, the λ repressor protein might recognize DNA through alternative codes.

This work was supported by a Patrick and Catherine Donaghue Foundation Biomedical research postdoctoral fellowship to D. C. Kombo and an NIGMS Traineeship in Molecular Biophysics to M. A. Young, from grant no. GM-08271 to Wesleyan University. Support was also received from grant no. GM-37909 from the National Institute of Health awarded to D. L. Beveridge. Molecular dynamics simulations were carried out using the Pittsburgh Supercomputer Center facility. Wesleyan University computer facility was used to analyze the MD

Table II Backbone Dihedral Angles[a] of Asn-52 Determined for Structures Averaged[b] over a 100 ps Range

Non-consensus Monomer		Consensus Monomer	
ϕ	φ	ϕ	φ
−96.6	9.2	−98.8	9.8
−99.1	1.8	−97.7	2.0
−106.1	1.1	−93.8	2.9
−110.9	6.7	−86.5	0.9
−98.5	−1.5	−83.3	−4.0
−105.4	−3.6	−85.7	−4.7
−87.6	−7.3	−79.1	−2.9
−87.2	−7.3	−79.8	−2.6
−87.2	−7.3	−85.5	−3.8
−76.9	−20.9	−85.6	−2.7

[a] In degrees.

[b] The values given in the first row refers to the starting configuration. From the second to the last row are given values that refer to the average structures obtained within 100–200, 200–300, . . .900–1000 ps, respectively.

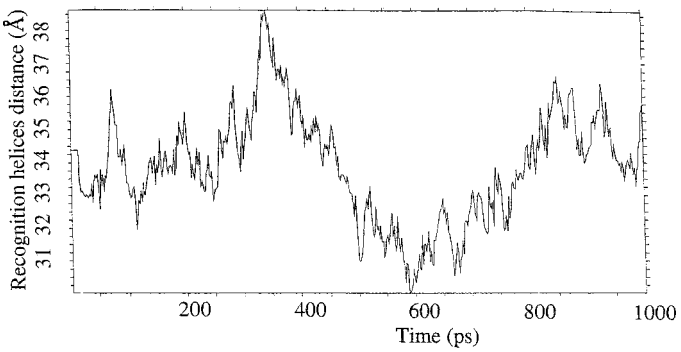

FIGURE 12 Time evolution of the distance of closest approach between the recognition helices (second helix of the helix–turn–helix in each monomer).

trajectory. We thank Drs. G. Ravishanker and B. Jayaram for reading the manuscript and very useful suggestions.

REFERENCES

1. Ptashne, M. A Genetic Switch: Gene Control and Phage λ: Cell Press; Cambridge, MA, and Blackwell, Palo Alto, CA, 1992.
2. Sauer, R. T.; Jordan, S. R.; Pabo, C. O. Adv Protein Chem 1990, 40, 1–61.
3. Pabo, C. O.; Lewis, M. Nature 1982, 298, 443–447.
4. Jordan, S. R.; Pabo, C. O. Science 1988, 242, 893–898.
5. Clark, N. D.; Beamer, L. J.; Goldberg, H. R.; Berkower, C.; Pabo, C. O. Science 1991, 254, 267–270.
6. Weiss, M. A.; Pabo, C. O.; Karplus, M.; Sauer, R. T. Biochemistry 1987, 23, 5090–5095.
7. Sarai, A.; Takeda, Y. Proc Nat Acad Sci USA 1989, 86, 6513–6517.
8. Sauer, R. T.; Hehir, K.; Stearman, R. S.; Weiss, M. A.; Jeitler-Nilsson, A.; Suchaneck, E. G.; Pabo, C. O. Biochemistry 1986, 25, 5992–5998.
9. Huang, Y. T.; Rusinova, E.; Ross, J. B. A.; Senear, D. F. J Mol Biol 1997, 267, 403–417.
10. Beamer, L. J.; Pabo, C. O. J Mol Biol 1992, 227, 177–196.
11. Benevides, J. M.; Weiss, M. A.; Thomas, G. J. J Biol Chem 1994, 269, 10869–10878.
12. Pabo, C. O.; Suchaneck, E. G. Biochemistry 1986, 25, 5987–5991.
13. Lee, C.; Levitt, M. Nature 1991, 352, 448–451.
14. Lee, C. J Mol Biol 1994, 236, 918–939.
15. Hellinga, H. W.; Richards, F. M. Proc Natl Acad Sci USA 1994, 91, 5803–5807.
16. Kombo, D. C.; Némethy, G.; Gibson, K. D.; Rackovsky, S.; Scheraga, H. A. J Mol Biol 1996, 256, 517–532.
17. Jayaram, B.; DiCapua, F. M.; Beveridge, D. L. J Am Chem Soc 1991, 113, 5211–5215.
18. Zacharias, M.; Luty, B. A.; Davis, M. E.; McCammon, J. A. Biophys J 1992, 63, 1280–1285.
19. Misra, V. K.; Hecht, J. L.; Sharp, K. A.; Friedman, R. A.; Honig, B. J Mol Biol 1994, 238, 264–280.
20. Cornell, W. D.; Ciepack, P.; Bayly, C. I.; Gould, I. R.; Merz, K. M., Jr.; Ferguson, D. M.; Spellmeyer, D. C.; Fox, T.; Cadwell, J. W.; Kollman, P. A. J Am Chem Soc 1995, 177, 5179–5197.
21. Kombo, D. C.; Young, M. A.; Beveridge, D. L. Proteins Struct Funct Genet 2000, in press.
22. Cheatham, T. E., III; Miller, J. L.; Fox, T.; Darden, T. A.; Kollman, P. A. J Am Chem Soc 1995, 117, 4193–4194.
23. Young, M. A.; Jayaram, B.; Beveridge, D. L. J Am Chem Soc 1996, 119, 59–69.
24. Ryckaert, J.-P.; Cicotti, B.; Berendsen, H. J. C. J Comp Phys 1977, 23, 327–341.
25. Ravishanker, G. Molecular Dynamics Toolchest, 1.0; Wesleyan University: Middletown, CT, 1991.
26. Biosym InsightII 2.2.0; Biosym Technologies: San Diego, CA, 1992.
27. Lim, W. A.; Hodel, A.; Sauer, R. T.; Richards, F. M. Proc Natl Acad Sci USA 1994, 91, 423–427.
28. Aggarwal, A. K.; Rodgers, D. W.; Drottar, M.; Ptashne, M.; Harrison, S. C. Science 1988, 242, 899–907.
29. Shimon, L. J. W.; Harrison, S. C. J Mol Biol 1993, 232, 826–838.
30. Rodgers, D. W.; Harrison, S. C. Structure 1993, 1, 227–240.
31. Schultz, S. C.; Shields, G. C.; Steitz, T. A. Science 1991, 253, 1001–1007.
32. Otwinowski, Z.; Schevitz, R. W.; Zhang, R.-G.; Lawson, C. L.; Joachimiack, A. J.; Marmorstein, R.; Luisi, B. F.; Sigler, P. B. Nature 1988, 335, 321–329.
33. Sklenar, H.; Etchebest, C.; Lavery, R. Proteins Struct Funct Genet 1989, 6, 46–60.
34. Ponder, J. W.; Richards, F. M. J Mol Biol 1987, 193, 775–791.
35. McGregor, M. J.; Islam, S. A.; Sternberg, J. E. J Mol Biol 1987, 198, 295–310.
36. McKay, D. B.; Steitz, T. A. Nature 1981, 290, 744–749.
37. Anderson, W. F., Ohlendorf, D. H.; Takeda, Y.; Matthews, B. W. Nature 1981, 290, 754–758.
38. Branden, C.; Tooze, J. Introduction to Protein Structure; Garland Publishing: New York, 1991.
39. Depouplana, L. R.; Auld, D. S.; Kim, S.; Schimmel, P. Biochemistry 1996, 35, 8095–8102.
40. Davis, D. Nature 1981, 290, 736–737.